Journal of Physics: Condensed Matter

PAPER

Real-space imaging of magnetic phase transformation in single crystalline Sm–Ca–Sr based manganite compound

To cite this article: Dipak Mazumdar *et al* 2021 *J. Phys.: Condens. Matter* **33** 235402

IOP Publishing Journal of Physics: Condensed Matter
J. Phys.: Condens. Matter **33** (2021) 235402 (6pp) https://doi.org/10.1088/1361-648X/abf6a7

Real-space imaging of magnetic phase transformation in single crystalline Sm–Ca–Sr based manganite compound

Dipak Mazumdar[1,*], Rajeev Rawat[2], Sanjib Banik[1,3], Kalipada Das[4] and I Das[1]

[1] Saha Institute of Nuclear Physics, HBNI, 1/AF, Bidhannagar, Kolkata 700 064, India
[2] UGC-DAE Consortium for Scientific Research, University Campus, Khandwa Road, Indore 425001, India
[3] Experimentelle Physik 3 (EP III), University of Wuerzburg, 97074 Wurzburg, Germany
[4] Seth Anandram Jaipuria College, 10 Raja Naba Krishna Street, Kolkata 700005, India

E-mail: dipak.mazumdar@saha.ac.in, dmazumdar2306@gmail.com and rrawat@csr.res.in

Received 29 January 2021, revised 13 March 2021
Accepted for publication 9 April 2021
Published 13 May 2021

Abstract

Low-temperature-high-magnetic field magnetic force microscopy studies on colossal magnetoresistance material $Sm_{0.5}Ca_{0.25}Sr_{0.25}MnO_3$ have been carried out. These measurements provide real-space visualization of antiferromagnetic–ferromagnetic (AFM–FM) transition on sub-micron length scale and explain the presence of AFM–FM transition in the temperature-dependent magnetization measurements, but the absence of corresponding metal–insulator transition in temperature-dependent resistivity measurements at the low magnetic field. Distribution of transition temperature over the scanned area indicates towards the quench disorder broadening of the first-order magnetic phase transition. It shows that the length scale of chemical inhomogeneity extends over several micrometers.

Keywords: magnetic phase transition, magnetic force microscopy, metal–insulator transition, colossal magnetoresistance material

(Some figures may appear in colour only in the online journal)

1. Introduction

Doped perovskite manganites having general formula $RE_{1-x}AE_xMnO_3$ (where RE and AE represent rare-earth and alkaline earth elements, respectively) show an intricate interplay of lattice, charge, and spin degrees of freedom, which give rise to nearly degenerate but contrasting magnetic and electronic states [1–6]. These states are susceptible to small perturbation which results in metal–insulator transition (MIT), colossal magnetoresistance (CMR) [7, 8], magnetocaloric effect [5, 9–11] etc. The ground state of these systems strongly depends on the bandwidth of the system e.g. narrow bandwidth systems order in a robust charge order antiferromagnetic insulator (CO-AF-I) state, whereas wide bandwidth systems order in a ferromagnetic metal (FM-M) state [12, 13]. The CO-AF-I state of narrow bandwidth half doped manganites like $Pr_{0.5}Ca_{0.5}MnO_3$ (PCMO), $Sm_{0.5}Ca_{0.5}MnO_3$ (SCMO) etc are highly insulating and require about 500 kOe magnetic field to melt it into a FM-M state, resulting in CMR [4, 12, 14]. Recently, a record high value of MR (10^{13}%) has been reported in polycrystalline $Sm_{0.5}Ca_{0.25}Sr_{0.25}MnO_3$ (SCSMO) by Banik *et al* [15].The compound can be considered as a derivative of SCMO (a narrow bandwidth system with robust CO-AF-I ground state) and $Pr_{0.5}Sr_{0.5}MnO_3$ (PSMO; a wide-bandwidth system with weak CO-AF-I state). As a result, zero-field cooled sate is highly insulating like SCMO, which is melted at much lower critical field like PSMO, resulting in CMR for a magnetic field of 20–30 kOe at liquid helium temperature. The magnetic behavior of this system is similar to Al-doped PCMO [16], PSMO [17], $Nd_{0.5}Sr_{0.5}MnO_3$ [18], $La_{0.5}Ca_{0.5}MnO_3$ [19, 20],

* Author to whom any correspondence should be addressed.

(LaPrCa)MnO_3 (LPCMO) [21–25] etc, where observed thermomagnetic irreversibility has been attributed to path-dependent AF-I and FM-M phase coexistent. Evidence of co-existing phases has been provided by several techniques including temperature-dependent magnetic force microscopy (MFM). These studies showed nucleation and growth of product phase over a wide temperature range [21, 24–27]. However, such MFM studies with temperature and magnetic field are few and more work is required in this direction to understand the nature of thermomagnetic irreversibility and the length scale of phase coexistence. Here, we report our MFM studies on single crystalline (SC) SCSMO at low temperature (down to 10 K) and high magnetic field, which brings out the history-dependent magnetic phase evolution on a mesoscopic length scale.

2. Experimental details

The SC-SCSMO sample studied in the present study is from the same ingot which had been used in the previous study [28]. The DC magnetization (M) measurements have been carried out using superconducting quantum interference device-vibrating sample magnetometer (SQUID-VSM) from M/s. Quantum design. Electrical resistivity (ρ) was measured in a cryogenic set-up using standard linear four-probe configuration in longitudinal geometry. MFM measurements have been performed on a mirror finished polished surface of SC-SCSMO using low-temperature-high-magnetic field (LTHM) fiber interferometer based AFM-MFM system from M/s. Attocube Systems AG, Germany and 90 kOe superconducting magnet system from M/s. American Magnetics, USA. All the images presented in this manuscript had been collected using the dual-pass mode, where the first pass measured topography and the second pass measured magnetic contrasts (as frequency shift Δf) with a lift off of 60 nm.

3. Results and discussions

Figure 1(a) shows the M vs T of SC-SCSMO, which is measured in the presence of 10 kOe magnetic field during zero-field cooled warming (ZFCW), field cooled cooling (FCC), and field cooled warming (FCW). A thermal hysteresis of about 16 K for FCC and FCW curves indicate a first-order antiferro–ferromagnetic (AF–FM) transition. The transformation taken as the temperature of minimum in dM/dT, are found to be 55 ± 13 K (T^*) during cooling and 71 K (T^{**}) during warming. The M values during ZFCW remain lower for $T < T^{**}$. On the other hand ρ–T (figure 1(b)) measured in the absence of applied magnetic field as well as in the presence of 20 kOe magnetic field shows an insulating behavior without any signature of MIT. The 20 kOe ρ curve follows zero-field curve but for $T < 50$ K, where $\rho(20\ \text{kOe}) < \rho(0\ \text{kOe})$. As highlighted in the inset, ln(ρ) varies linearly with $T^{-1/4}$ in the absence of an applied magnetic field, which indicates a variable range hopping conduction mechanism. For ρ(20 kOe), a deviation can be noticed below 40 K. The observed ρ behavior is similar to that observed in the case of LPCMO thin

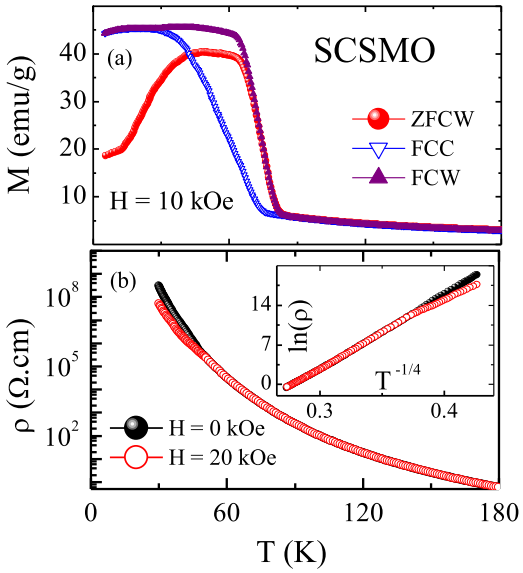

Figure 1. (a) Temperature dependence of magnetization (M) of SC-SCSMO measured during ZFCW, FCC, and FCW in the presence of a 10 kOe magnetic field. (b) The temperature dependence of resistivity (ρ) of SCSMO-SC measured in 0 kOe and 20 kOe applied magnetic field. Linear ln(ρ) vs $T^{-1/4}$ in the inset highlights variable range hopping conduction mechanism in the absence of applied magnetic field and deviation from it at low temperature in the presence of 20 kOe.

film above its MIT [21]. There, an apparent change in transport mechanism has been identified with the nucleation and growth of the FM-M phase in the insulating AF-I matrix on a sub-micron length scale. For a detailed understanding of the change of magnetic ground state upon application of the magnetic field, isothermal resistivity measurement at $T = 2$ K has been performed (as shown in figure 2). The flat region in the $\rho(T)$ curve, formed due to the CO-AF-I state existed below a critical field (H_C) value of around 30 kOe. A higher magnetic field above H_C helps to melt this robust CO-AF-I state into an FM-M state and the system settled down to a low resistive state even after removal of the magnetic field. In addition to it, abrupt insulator to metal transition in the virgin curve is prominent. Abrupt resistivity change with magnetic field has been reported initially in the isothermal magnetoresistance data of $Nd_{0.5}Sr_{0.5}MnO_3$ single crystal by Kuwahara *et al* [29]. Subsequently, similar feature in isothermal ρ–H and M–H measurement has been reported for several other manganite single crystal as well as polycrystals [15, 29–35]. These studies bring out that the discontinuous transitions are observed at low temperature (typically less than 5 K), critical field for triggering the transition depend on field sweep rate as well as cooling history of the sample, and transition is accompanied with momentary increase of sample temperature. The origin of abrupt transformation remains unclear with possible explanations; strain between co-existing phases, orbital frustration, blocked metastable states etc. The latter explanation gains support from the fact that such abrupt transitions are not limited to manganite and has been observed in a wide variety of systems e.g. Ta doped $HfFe_2$ [36, 37], $LaFe_{12}B_6$ [38], Nd_7Rh_3 [39], doped $CeFe_2$ [40]. Common ingredient among all these systems

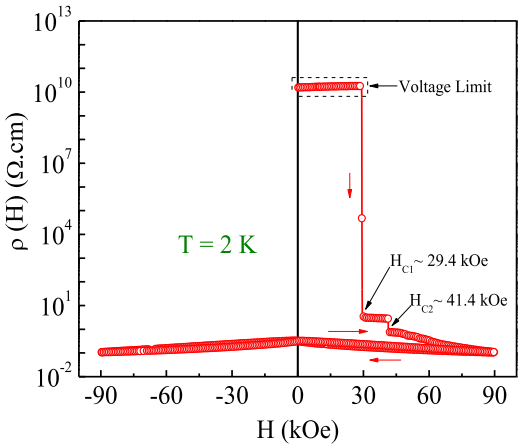

Figure 2. Variation of electrical resistivity (ρ) with external magnetic field (H) measured after zero field cooling at $T = 2$ K.

is the quench disorder broadened first-order phase transition and presence of kinetically arrested metastable magnetic state at low temperature.

Since aim of present investigation was the study of phase co-existence across magnetic transition therefore MFM measurements were carried out for $T \geqslant 10$ K, at which transition becomes less abrupt and provide a reasonable magnetic field window to observe co-existing phases. The field-induced transition in M–H and MFM measurement is shown in figure 3 at 10 K. For these measurements, the sample was cooled under zero field to 10 K and magnetic field was applied isothermally at 10 K. Magnetization (M) varies almost linearly with an increase in magnetic field up to 20 kOe and shows a field-induced transition to FM state with further increase in the magnetic field. The transition appears to continues up to 70 kOe, the maximum field available with SQUID-VSM. With reducing magnetic field, M remains nearly constant down to 10 kOe and then decreases rapidly to zero. MFM images along with its histogram of the frequency shift are shown for the labeled magnetic field value and direction (indicated by the red star in the M–H curve). The MFM image at 10 K before the application of the magnetic field (image (a)) shows negligible Δf, which is consistent with AF state for ZFC sample in bulk magnetization measurements [15]. The MFM images within 5–35 kOe are found to be almost independent of the magnetic field and one typical image is shown as image (b). It shows uniform contrast with some line-like features. The contrast in the MFM images start to change at 40 kOe (image (c)), where dark region at the bottom left corner indicates the growth of the FM region. With further increase in magnetic field, the dark region expands and almost 50% area of the image at 50 kOe (image (d)) and covers almost complete image at 60 kOe (image (e)). The presence of line-like features in otherwise uniform contrast at 60 kOe (image (e)) is almost identical to that observed at 10 kOe i.e. image (b). Therefore, these features may be attributed to crack or some impurity phases, beneath the sample surface. With reducing magnetic field the MFM images remain unchanged down to 10 kOe (image (f)). The contrast in the image (g), which, is measured at 0 kOe after field cycling at 10 K, shows an almost equal distribution of dark and light regions. Here, contrast variation can be attributed to randomly oriented FM domains of a few micrometer sizes. It is supported by the fact that this contrast vanishes with the application of a small magnetic field e.g. see the first image in figure 4 corresponds to $T = 10$ K, $H = 20$ kOe measured immediately after magnetic field cycling at 10 K. The overall frequency shift for this image is 154 Hz, which is close to image (f) in figure 3. This experiment shows that FM phase grows at the expense of AF phase with increase in magnetic field and within the transition window FM and AF phase co-exist on a micrometer length scale.

The thermal evolution of the field-induced FM state at 10 K (obtained after field cycling in figure 3), is studied during warming in the presence of 20 kOe magnetic field. The measurement is carried out immediately after the isothermal field cycling measurement discussed above i.e. 20 kOe magnetic field is applied again after field cycling 0–70–0 at 10 K. As discussed above, the MFM image at 10 K in figure 4 represents almost FM state. The contrast remains unchanged up to 40 K indicating that field-induced FM state is retained up to this temperature. Transition to AF state can be observed around 60 K, which shows the presence of nearly equal area corresponding to the dark and light region. At 65 K, isolated dark regions of few micron sizes with much smaller Δf are observed and finally at 70 K Δf variation becomes negligible. Though the scanned area in these images are not exactly identical, it can be inferred that regions which showed field-induced transition to FM state around 40–60 kOe at 10 K transform to AF state on warming in the temperature range 60–65 K in the presence of 20 kOe magnetic field.

The results of MFM and M–T measurement during FCC and FCW in the presence of a 20 kOe magnetic field are shown in figure 5. During FCC, FM nuclei of a few micrometer sizes appear around 35 K. The regions grow in size along with the appearance of new FM regions at 25 K and this state remains nearly unchanged with further cooling to 15 K. The sample is warmed from 15 K to 25 K and left for 12 h. In contrast to 25 K and 15 K images during cooling, it shows additional FM regions, which brings out the extremely slow nature of AF to FM transformation at low temperature. The MFM images remain nearly unchanged on further warming up to 60 K. At 65 K, a small FM circular region of a few micron diameters appears to be at the same position at which, the FM region appeared during cooling around 35 K. Finally contrast vanishes again at 70 K. The occurrence of AF to FM transition in the form of isolated, non-percolative FM region explains the presence of FM–AF transition in M–T, but the absence of corresponding MIT in ρ–T measurements.

These results can be explained in the framework of broadening of first order transition due to quench disorder [43, 44]. One inherent source of quench disorder is chemical inhomogeneity in doped compound. Several reports on the effect of quenched disorder and phase coexistence on the modification of the ground state of half-doped manganites are already documented in the literature [15–18, 21, 26, 27, 41–47]. For example, the strength of charge-ordering in the narrow bandwidth PCMO system is systematically weaken when the doping concentration of Al on the Mn-site increases and ferromagnetic clusters

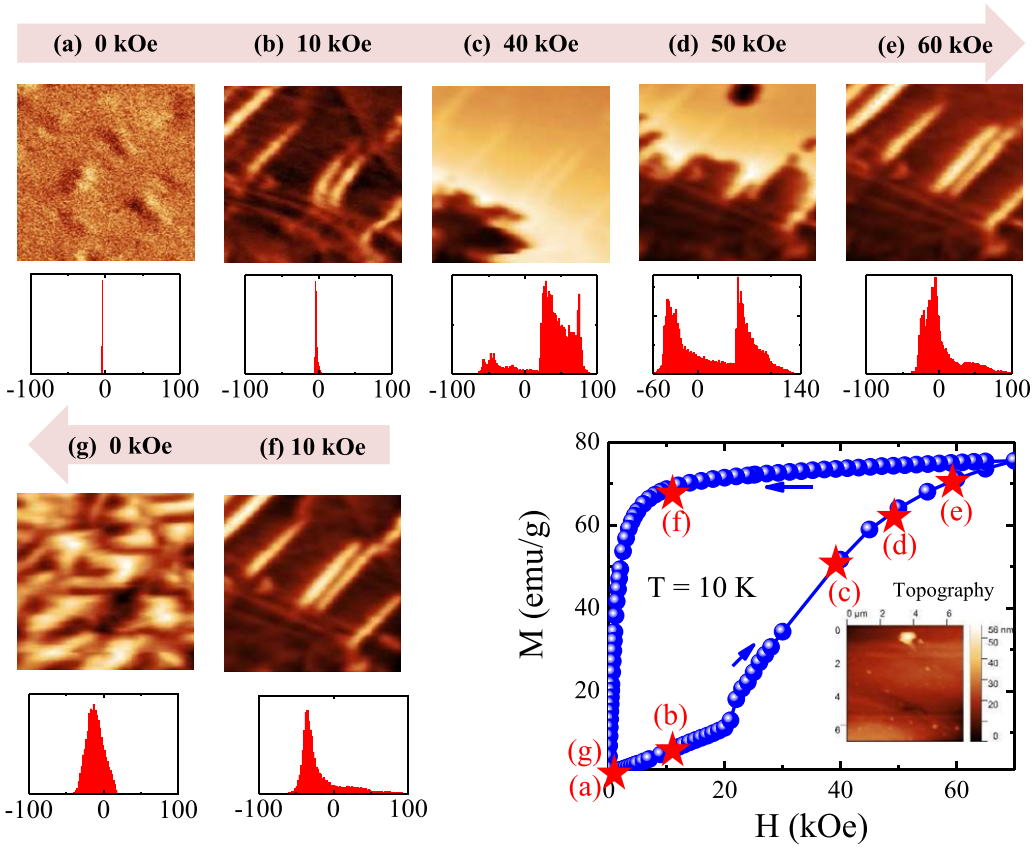

Figure 3. Isothermal MFM and bulk magnetization (M) measurement showing field induced AF–FM transition at 10 K for a zero-field cooled SCSMO single crystal. Each MFM image represents an area of 7 μm $\times$ 7 μm of the sample. The histogram below the MFM image show distribution of frequency shift (Δf on x-axis and y-axis is count normalized to 1). The red stars in the M vs H plot mark the field values at which MFM images were measured.

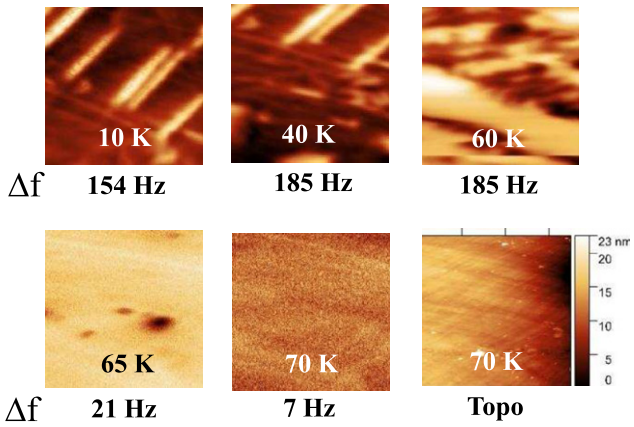

Figure 4. MFM images of SCSMO single-crystal taken during warming in the presence of 20 kOe magnetic field. These images were measured immediately after isothermal field cycling measurement shown in figure 3. Each MFM image represent an area of 7 μm $\times$ 7 μm and range of color scale (Δf) are written below the respective MFM image, where dark color represent higher frequency shift.

with finite-size formed due to the presence of quenched disorder in the system [16, 26, 41]. The effect of quenched disorder on the physical properties can also be observed in larger bandwidth manganite systems like $Nd_{0.5}Sr_{0.5}MnO_3$ [42]. As stated in the introduction, the system under study can be considered as a solution of SCMO and $Sm_{0.5}Sr_{0.5}MnO_3$. The lattice mismatch due to Ca and Sr doping affects the Mn–O bond lengths and $\langle$Mn–O–Mn$\rangle$ bond angles, and therefore one-electron bandwidth of the system. As a result substitution of Sr for Ca result in weakening of CO, which is evidenced from lower critical field required for melting of CO with increase in Ca concentration [48]. An inhomogeneity in Ca and Sr on the length scale of correlation length can lead to different critical field for different regions of the sample. For a macroscopic sample, therefore transition will occur over a magnetic field range. In a two-parameter (H, T) space it implies that otherwise sharp transition line for an ideal first-order magnetic transition becomes a band made up of quasicontinuum of lines, each representing a region of the sample [21, 27, 44–46]. This is shown schematically at the bottom of figure 5, which represents the band corresponding to transformation during cooling/field increasing (H^*, T^*) and warming/field decrease (H^{**}, T^{**}). Since the transition takes place from low-T FM to a high-T AF state, the slopes of these bands are positive. From this diagram, it is evident that the region which transforms at lower T (dark color) with temperature sweep, requires higher H for field-induced transformation. The MFM images measured during isothermal field cycling (along the path BC) showed transition around 40–50 kOe at 10 K in figure 3.

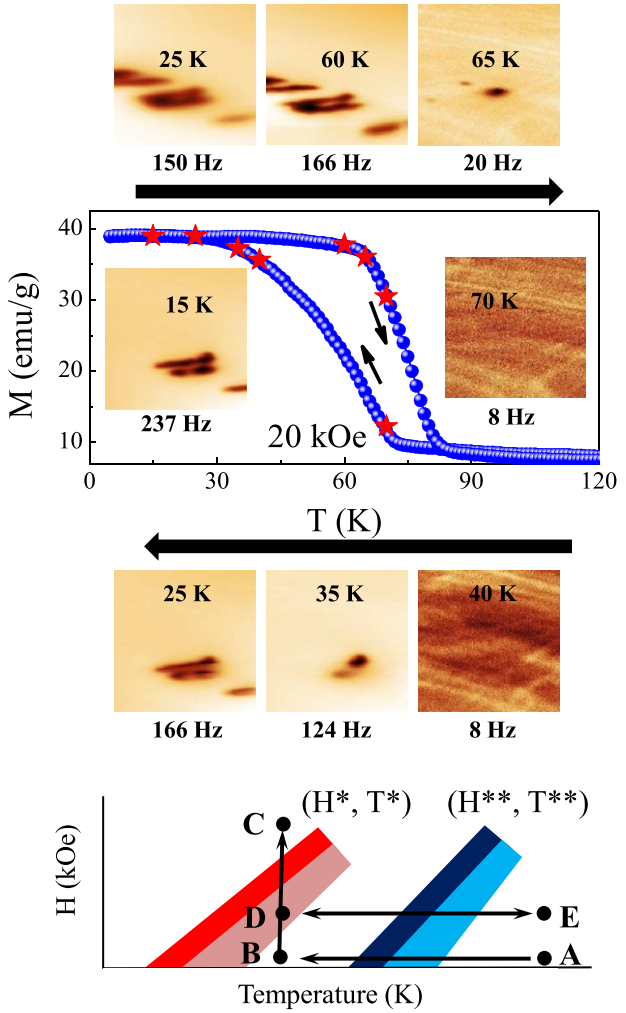

Figure 5. MFM images and bulk magnetization (M) of SCSMO single crystal measured during FCC and subsequent warming (FCW). The red stars in the MFM image correspond to the temperatures of the MFM images shown in the figure. Each MFM image represent an area of 7 μm $\times$ 7 μm and range of color scale (Δf) are written below respective MFM image, where dark color represent higher frequency shift. Schematic (H, T) phase diagram of disorder broadened first-order transition of the present sample, where AF to FM transition occurs across (H^*, T^*) band and FM to AF transition occurs across (H^{**}, T^{**}) band. Solid arrows represent the path followed for MFM measurement presented in this manuscript. See text for details.

This window is much smaller and lies toward the higher field side of 20–60 kOe transition window observed in bulk M–H measurement i.e. studied region in the MFM measurement in figure 3 corresponds to darker region of the (H^*, T^*) band in figure 5. As expected, with an increase in temperature (path DE) these field-induced FM regions transform into AF state at lower temperature side of T^{**} band (dark blue band) or within 60–65 K then the bulk sample (60–80 K). During FCC in the presence of 20 kOe, only a small fraction of (H^*, T^*) band is crossed therefore only a few FM region are observed during cooling. The identical nucleation and annihilation position of FM nuclei during FCC (at 35 K) and FCW (at 65 K) conforms to the transition distribution due to quench disorder broadening. The fact that the transition width in MFM measurements are much smaller (about 30%) than that observed in bulk magnetization measurement, it suggests that the length scale of chemical inhomogeneity is much larger than 7 micro-meter.

4. Conclusions

To conclude, the path-dependent LTHM-MFM measurement shows phase co-existence over a length scale of sub-micrometer to several micrometers. These measurements bring out transition temperature variation over the scanned area, which can be attributed to the compositional fluctuation inherent in substitutional alloys. Transformation from AF to FM state occurs within the field range 40–60 kOe at 10 K in contrast to 20–70 kOe observed in the bulk measurement. Similarly, the FM phase obtained after field cycling transform to AF state in the temperature range 60–65 K in contrast to 60–80 K during warming in the presence of 20 kOe magnetic field. The nucleation of growth of isolated FM region explains the presence of FM–AF transition in MT but its absence in ρ–T measurement. The growth of the FM region with time (about 12 h) brings out the metastable nature of the co-existing magnetic state, which will require further measurements.

Data availability statement

The data that support the findings of this study are available upon reasonable request from the authors.

Acknowledgments

The authors would like to thank Dept. of Atomic Energy, Govt. of India for financial assistance.

ORCID iDs

Dipak Mazumdar https://orcid.org/0000-0001-7975-2819
Rajeev Rawat https://orcid.org/0000-0003-3120-3276
Sanjib Banik https://orcid.org/0000-0002-4143-9664
Kalipada Das https://orcid.org/0000-0001-7895-518X

References

[1] Tokura Y 2000 *Colossal Magnetoresistive Oxides* (London: Gordon and Breach)
[2] Dagotto E 2005 *Science* **309** 257
Mathur N and Littlewood P 2003 *Phys. Today* **56** 25
[3] Phan M H, Morales M B, Bingham N S, Srikanth H, Zhang C L and Cheong S W 2010 *Phys. Rev.* B **81** 094413
[4] Biswas A and Das I 2006 *Phys. Rev.* B **74** 172405
[5] Guo Z B, Du Y W, Zhu J S, Huang H, Ding W P and Feng D 1997 *Phys. Rev. Lett.* **78** 1142
[6] Guo Z B, Zhang J R, Huang H, Ding W P and Du Y W 1997 *Appl. Phys. Lett.* **70** 904
[7] Jin S, Tiefel T H, McCormack M, Fastnacht R A, Ramesh R and Chen L H 1994 *Science* **264** 413

[8] Uehara M, Mori S, Chen C H and Cheong S-W 1999 *Nature* **399** 560
[9] Phan M-H and Yu S-C 2007 *J. Magn. Magn. Mater.* **308** 325
[10] Biswas A, Samanta T, Banerjee S and Das I 2008 *Appl. Phys. Lett.* **92** 012502
[11] Gschneidner K A Jr, Pecharsky V K and Tsokol A O 2005 *Rep. Prog. Phys.* **68** 1479
[12] Tokura Y 2006 *Rep. Prog. Phys.* **69** 797
[13] Sen C, Alvarez G and Dagotto E 2007 *Phys. Rev. Lett.* **98** 127202
[14] Tokura Y and Tomioka Y 1999 *J. Magn. Magn. Mater.* **200** 1
[15] Banik S, Das K, Paramanik T, Lalla N P, Satpati B, Pradhan K and Das I 2018 *NPG Asia Mater.* **10** 923
[16] Nair S and Banerjee A 2004 *J. Phys.: Condens. Matter.* **16** 8335
[17] Pramanik A K and Banerjee A 2008 *J. Phys.: Condens. Matter.* **20** 275207
[18] Rawat R, Mukherjee K, Kumar K, Banerjee A and Chaddah P 2007 *J. Phys.: Condens. Matter.* **19** 256211
[19] Zhou H, Wang L, Hou Y, Huang Z, Lu Q and Wu W 2015 *Nat. Commun.* **6** 8980
[20] Zhou H B, Hou Y B and Lu Q Y 2015 *Chin. J. Chem. Phys.* **28** 6
[21] Rawat R, Kushwaha P, Mishra D K and Sathe V G 2013 *Phys. Rev.* B **87** 064412
[22] Rawat R, Sathe V G and Chaddah P 2017 arXiv:1712.06345v1
[23] Burkhardt M H *et al* 2012 *Phys. Rev. Lett.* **108** 237202
[24] Zhang L, Israel C, Biswas A, Greene R L and de Lozanne A 2002 *Science* **298** 805
[25] Wu W, Israel C, Hur N, Park S, Cheong S-W and de Lozanne A 2006 *Nat. Mater.* **5** 881
[26] Lakhani A, Kushwaha P, Rawat R, Kumar K, Banerjee A and Chaddah P 2010 *J. Phys.: Condens. Matter.* **22** 032101
[27] Manekar M A, Chaudhary S, Chattopadhyay M K, Singh K J, Roy S B and Chaddah P 2001 *Phys. Rev.* B **64** 104416
[28] Mazumdar D, Das K, Roy S and Das I 2020 *J. Magn. Magn. Mater.* **497** 166066
[29] Kuwahara H, Tomioka Y, Asamitsu A, Moritomo Y and Tokura Y 1995 *Science* **270** 961
[30] Mahendiran R, Maignan A, Hebert S, Martin C, Hervieu M, Raveau B, Mitchell J F and Schiffer P 2002 *Phys. Rev. Lett.* **89** 286602
[31] Fisher L M, Kalinov A V, Voloshin I F, Babushkina N A, Khomskii D I, Zhang Y and Palstra T T M 2004 *Phys. Rev.* B **70** 212411
[32] Hardy V *et al* 2004 *Phys. Rev.* B **69** 020407
[33] Ghivelder L *et al* 2004 *Phys. Rev.* B **69** 214414
[34] Ghivelder L, Eslava G G, Freitas R S, Leyva G and Parisi F 2016 *J. Alloys Compd.* **680** 494
[35] Matsukawa M *et al* 2007 *Phys. Rev. Lett.* **98** 267204
[36] Rawat R, Chaddah P, Bag P, Babu P D and Siruguri V 2013 *J. Phys.: Condens. Matter.* **25** 066011
[37] Reddy V R, Rawat R, Gupta A, Bag P, Siruguri V and Chaddah P 2013 *J. Phys.: Condens. Mater.* **25** 316005
[38] Diop L V B, Isnard O and Rodriguez-Carvaja J 2016 *Phys. Rev.* B **93** 014440
[39] Sengupta K and Sampathkumaran E V 2006 *Phys. Rev.* B **73** 020406
[40] Roy S B, Chattopadhyay M K, Chaddah P and Nigam A K 2005 *Phys. Rev.* B **71** 174413
[41] Nair S and Banerjee A 2004 *Phys. Rev. Lett.* **93** 117204
[42] Wakabayashi Y, Bizen D, Nakao H, Murakami Y, Nakamura M, Ogimoto Y, Miyano K and Sawa H 2006 *Phys. Rev. Lett.* **96** 017202
[43] Imry Y and Wortis M 1979 *Phys. Rev.* B **19** 3580
[44] Kumar K, Pramanik A K, Banerjee A, Chaddah P, Roy S B, Park S, Zhang C L and Cheong S-W 2006 *Phys. Rev.* B **73** 184435
[45] Kushwaha P, Rawat R and Chaddah P 2008 *J. Phys.: Condens. Matter.* **20** 022204
[46] Rawat R, Chaddah P, Bag P, Das K and Das I 2012 *J. Phys.: Condens. Matter.* **24** 416001
[47] Sathe V G, Ahlawat A, Rawat R and Chaddah P 2010 *J. Phys.: Condens. Matter.* **22** 176002
[48] Banik S, Pradhan K and Das I 2021 *J. Alloys Compd.* **862** 158515